Downregulation of growth arrest-specific transcript 5 alleviates palmitic acid-induced myocardial inflammatory injury through the miR-26a/HMGB1/NF-κB axis

QINGXIONG YUE[1], CUITING ZHAO[1], YONGHUAI WANG[1], LANTING ZHAO[1],
QING ZHU[1], GUANGYUAN LI[1], NAN WU[2], DALIN JIA[3] and CHUNYAN MA[1]

[1]Department of Cardiovascular Ultrasound; [2]The Core Laboratory; [3]Department of Cardiology,
The First Affiliated Hospital of China Medical University, Shenyang, Liaoning 110001, P.R. China

Abstract. Palmitic acid (PA) can induce lipotoxic damage to cardiomyocytes, although its precise mechanism of action has not been completely elucidated. Growth arrest-specific transcript 5 (GAS5) is a long noncoding RNA that serves a regulatory role in several pathological processes, including tumorigenesis, stroke, cardiac fibrosis and osteoarthritis; however, its role in PA-induced myocardial injury remains elusive. The present study aimed to explore the role and underlying mechanism of GAS5 on PA-induced myocardial injury. The expression of GAS5 in PA-treated cardiomyocytes (H9c2 cells) was detected by reverse transcription-quantitative polymerase chain reaction (RT-qPCR), and its effects on PA-induced myocardial injury were measured by Cell Counting Kit-8 and lactate dehydrogenase (LDH) assays. The activities of cytokines and nuclear factor (NF)-κB were also detected by enzyme-linked immunosorbent assay, while interactions between GAS5 and microRNA (miR)-26a were evaluated by luciferase reporter assay and RT-qPCR. The regulation of GAS5 on high mobility group box 1 (HMGB1) expression was detected by RT-qPCR and western blotting. The results demonstrated that GAS5 was significantly upregulated in cardiomyocytes following treatment with PA. GAS5-knockdown increased the viability of PA-treated cardiomyocytes and reduced the activity of LDH, tumor necrosis factor-α and interleukin-1β. Furthermore, the present study identified that GAS5 specifically binds to miR-26a, and a reciprocal negative regulation exists between the two. The present study also demonstrated that GAS5 downregulation inhibited HMGB1 expression and NF-κB activation, while these suppressive effects were mediated by miR-26a. In conclusion, the present study demonstrated that PA can induce GAS5 expression and that the downregulation of GAS5 alleviated PA-induced myocardial inflammatory injury through the miR-26a/HMGB1/NF-κB axis. These data may provide a novel insight into the mechanism of myocardial lipotoxic injury.

Introduction

Owing to changes in lifestyle and dietary structure in modern society, the incidence of obesity has gradually increased worldwide (1). Obesity, a lipid metabolism disorder, can lead to an elevated level of free fatty acids (FFAs) (2), which have been reported to be associated with an increased risk and severity of heart failure (3). Furthermore, our previous study (4) and other researchers (5,6) have demonstrated that palmitic acid (PA), a major component of FFAs, significantly reduces the viability of cardiomyocytes and induces myocardial injury *in vitro* and *in vivo*. Therefore, PA-induced myocardial injury is considered to be one of the factors contributing to obesity-induced impairment of the heart. However, the mechanism of PA-induced myocardial injury has not been completely elucidated.

A long noncoding RNA (lncRNA) is defined as an RNA transcript of >200 nucleotides in length that regulates gene expression at multiple levels (7). For instance, the lncRNAs H19 (8) and X-inactive specific transcript (Xist) (9) are involved in genomic imprinting, which is a type of epigenetic regulation. Furthermore, the lncRNA PANDA participated in transcriptional regulation via a molecular decoy (10). In addition, an increasing number of lncRNAs have been reported to regulate gene expression at the post-transcriptional level as a competitive endogenous RNA (ceRNA) (11-13). Therefore, lncRNAs may provide novel insight into the underlying mechanism of PA-induced myocardial injury.

Growth arrest-specific transcript 5 (GAS5) is a well-known lncRNA that was initially identified in mouse

Correspondence to: Dr Chunyan Ma, Department of Cardiovascular Ultrasound, The First Affiliated Hospital of China Medical University, 155 North Nanjing Street, Heping, Shenyang, Liaoning 110001, P.R. China
E-mail: mcy_echo@163.com

Dr Dalin Jia, Department of Cardiology, The First Affiliated Hospital of China Medical University, 155 North Nanjing Street, Heping, Shenyang, Liaoning 110001, P.R. China
E-mail: jdl2001@126.com

NIH 3T3 cells (14). GAS5 has been reported to be involved in multiple pathological processes, including tumorigenesis and metastasis (15,16), ischemic stroke (17), hepatic and cardiac fibrosis (18,19), and the development of osteoarthritis (20). Notably, several lncRNAs have been reported to be involved in lipotoxicity. For instance, metastasis-associated lung adenocarcinoma transcript 1 promotes PA-induced lipid accumulation in hepatocytes by increasing the stability of the sterol regulatory element binding transcription factor 1 protein (21), while growth arrested DNA-damage inducible gene 7 is a key regulator of PA-induced oxidative stress and cell death in cultured fibroblasts (22). However, whether GAS5 serves a role in PA-induced myocardial injury remains elusive.

The aim of the present study was to explore the role of GAS5 in PA-induced myocardial injury and its underlying mechanism of action. The results demonstrated that GAS5 was significantly upregulated in cardiomyocytes following treatment with PA, while knockdown of GAS5 expression alleviated PA-induced myocardial injury and inflammatory activation. Mechanistically, GAS5 was identified to act as a ceRNA to regulate high mobility group box 1 (HMGB1) expression by binding with microRNA (miR)-26a, subsequently inhibiting nuclear factor (NF)-κB activation.

Materials and methods

Cell culture and PA treatment. The rat myocardial H9c2 cell line was obtained from the Shanghai Institutes for Biological Sciences (Shanghai, China). Cells were grown in Dulbecco's modified Eagle's medium (Gibco; Thermo Fisher Scientific, Inc., Waltham, MA, USA) supplemented with 10% fetal bovine serum (TBD Science, Tianjin, China), 100 units of penicillin/ml and 100 μg of streptomycin/ml in a humidified atmosphere at 37°C with 5% CO_2. H9c2 cells were treated with 400 μM PA (Sigma-Aldrich; Merck KGaA, Darmstadt, Germany) for consecutive 6, 12 or 24 h to induce myocardial lipotoxic injury according to the previously published study (4).

Oil Red O staining. Following the aforementioned treatment with PA for 24 h, cells were fixed in 4% paraformaldehyde for 30 min at room temperature. Following washing three times with phosphate-buffered saline, cells were incubated with 3 mg/ml Oil Red O working solution (Sigma-Aldrich; Merck KGaA) for 30 min at room temperature. Cell nuclei were then stained with hematoxylin for 2 min at room temperature, followed by imaging with a light microscope (Olympus Corporation, Tokyo, Japan).

Cell transfection. GAS5-specific small interfering RNA (siRNA) (sense, 5'-TCTCACAGGCAGTTCTGTGG-3', antisense, 5-ATCCATCCAGTCACCTCTGG-3'), scrambled siRNA [serving as the negative control (NC)], (sense, 5'-UUC UCCGAACGUGUCACGUTT-3', antisense, 5-ACGUGA CACGUUCGGAGAATT-3') miR-26a mimics (5'-UUCAAG UAAUCCAGGAUAGGCU-3'), mimics NC (5'-UUCUCC GAACGUGUCACGUTT-3'), miR-26a inhibitor (5'-AGC CTATCCTGGATTACTTGAA-3') and inhibitor NC (5'-CAG UACUUUUGUGUAGUACAA-3') were designed and synthesized by Shanghai GenePharma Co., Ltd. (Shanghai, China). Briefly, cells were transfected with the 5 μl siRNAs (20 μM)

and 200 μl miRNA nucleotide sequences (100 nM) using Lipofectamine® 2000 (Invitrogen; Thermo Fisher Scientific, Inc.) according to the manufacturer's protocol. At 24 h post-transfection, cells were then washed and cultured in fresh medium, followed by treated with 400 μM PA for 24 h.

Reverse transcription-quantitative polymerase chain reaction (RT-qPCR). Total RNA was extracted from the cells using TRIzol reagent (Invitrogen; Thermo Fisher Scientific, Inc.) according to the manufacturer's protocol. RNA concentration and A260/280 was measured using a NanoPhotometer P-Class (Implen GmbH, Munich, Germany). To detect mRNA expression levels, the PrimeScript RT reagent kit with gDNA Eraser (Takara Bio, Inc., Otsu, Japan) and SYBR Premix Ex Taq II (Takara Bio, Inc.) were used for RT and qPCR, respectively, according to the manufacturer's protocol. To detect miR-26a expression, Mir-X™ miRNA First Strand Synthesis kit and Mir-X™ miRNA RT-qPCR SYBR® kit (Takara Bio, Inc., Otsu, Japan) were used for RT and qPCR, respectively, according to the manufacturer's protocol. PCR was performed at 42°C for 30 min; 95°C for 10 min, followed by 45 cycles of amplification at 95°C for 20 sec, 62°C for 30 sec, 72°C for 30 sec. The melt curve stage was performed at 95°C for 15 sec, 60°C for 1 min, 95°C for 15 sec. GAPDH and U6 were used as the internal controls in the detection of mRNA and miRNA expression levels. All oligonucleotide primers were designed by Shanghai Sangon Biotech Co., Ltd. (Table I). The relative expression was analyzed using $2^{-\Delta\Delta Cq}$ method (23).

Cell Counting Kit (CCK)-8 assay. Cells were seeded at $5x10^3$ cells/well in 96-well plates. Following transfection for 24 h, the cell viability was determined by CCK-8 assay (Dojindo Molecular Technologies, Inc., Kumamoto, Japan) according to the manufacturer's protocol. The absorbance value was detected at 450 nm by an Epoch 2 Microplate Spectrophotometer (BioTek Instruments, Inc., Winooski, VT, USA).

Lactate dehydrogenase (LDH) assay. Cells were seeded at $1x10^5$ cells/well in 24-well plates. Following transfection for 24 h, LDH released from the cardiomyocytes into the culture medium was measured using an LDH assay kit (cat. no. A020-1; Nanjing Jiancheng Bioengineering Institute, Nanjing, China) according to the manufacturer's protocol. The absorbance value was detected at 450 nm by an Epoch 2 Microplate Spectrophotometer (BioTek Instruments, Inc., Winooski, VT, USA).

Enzyme-linked immunosorbent assay (ELISA) for measuring cytokine and NF-κB activities. Cells were seeded at $1x10^5$ cells/well in 24-well plates. Following transfection for 24 h, the concentrations of tumor necrosis factor α (TNF-α) and interleukin-1β (IL-1β) in the culture medium were detected using commercial rat TNF-α or IL-1β ELISA kits (cat. no. EK3822/2 and EK301B2/2, respectively; Hangzhou MultiSciences Biotech Co., Ltd., Hangzhou, China) according to the manufacturer's protocol. To measure the activity of NF-κB, cells were harvested after transfection and PA treatment, and nuclear extract lysates were extracted from harvested cells using Nuclear Extraction kit (cat. no. ab113474; Abcam, Cambridge, UK), according to the manufacturer's protocol. The

Table I. Primer sequences.

Name	Sequences (5'-3')
GAS5	Forward: TCTCACAGGCAGTTCTGTGG
	Reverse: ATCCATCCAGTCACCTCTGG
TNF-α	Forward: GAAGAGAACCTGGGAGTAGATAAGG
	Reverse: GTCGTAGCAAACCACCAAGC
IL-1β	Forward: TCGTTGCTTGTCTCTCCTTG
	Reverse: AAAAATGCCTCGTGCTGTCT
HMGB1	Forward: CAAACCTGCCGGGAGGAGCA
	Reverse: TCTTTCATAACGAGCCTTGTCAGCC
GAPDH	Forward: ATCATCAGCAATGCCTCC
	Reverse: CATCACGCCACAGTTTCC
miR-26a	RT: CTCAACTGGTGTCGTGGAGTCGGCAATTCAGTTGAGACCCAG
	Forward: AAGGAGAACCCGTAGATCCG
	Reverse: GTGCAGGGTCCGAGGTATTC

GAS5, growth arrest-specific transcript 5; TNF-α, tumor necrosis factor α; IL-1β, interleukin-1β; HMGB1, high mobility group box 1; RT, reverse transcription.

activity of NF-κB in nuclear extract lysates was detected using NF-κB p65 transcription factor assay kit (cat. no. ab133112; Abcam) according to the recommended experimental protocol.

Bioinformatics analysis. starBase v2.0 (http://starbase. sysu.edu.cn/index.php) and LncBase Predicted v.2 tool (http://carolina.imis.athena-innovation.gr/diana_tools/web/index.php?r=lncbasev2/index-predicted) were employed to predict the binding cites between GAS5 and miRNAs.

Luciferase activity assay. Luciferase reporter plasmids (pmirGLO-GAS5-wt and pmirGLO-GAS5-mut) were obtained from Shanghai GenePharma Co., Ltd. Briefly, $2x10^5$ cells were plated into each well of a 24-well plates and transfected with pmirGLO-GAS5-wt or pmirGLO-GAS5-mut together with miR-26a mimics or mimics NC, as previously described (18). At 48 h post-transfection, luciferase activity was analyzed using the Dual-Glo Luciferase assay system (Promega Corporation, Madison, WI, USA) according to the manufacturer's protocol.

Western blotting analysis. Total proteins were extracted with RIPA buffer (Beyotime Institute of Biotechnology, Shanghai, China). The nuclear and cytoplasmic proteins were separately extracted using Nuclear and Cytoplasmic Protein Extraction kit (Beyotime Institute of Biotechnology), according to the manufacturer's protocol, and the protein concentration was measured by Enhanced BCA Protein Assay kit (Beyotime Institute of Biotechnology), according to the manufacturer's protocol. Next, 50 μg heat-denatured proteins were separated by 8% or 10% SDS-PAGE and then transferred to polyvinylidene difluoride membranes, followed by blocking with 1% bovine serum albumin solution at room temperature for 1 h. The membranes were then incubated at 4°C overnight with primary antibodies, including anti-HMGB1 (cat. no. ab128129; 1:1,000; Abcam), anti-NF-κB p65 (cat. no. ab193238; 1:1,000;

Abcam), anti-GAPDH (cat. no. TA336768; 1:1,000; Zhongshan Jinqiao Biotechnology, Beijing, China) and anti-Lamin A (cat. no. ab26300; 1:1,000; Abcam), followed by incubation with horseradish peroxidase conjugated goat anti-rabbit or goat anti-mouse immunoglobulin G (cat. no. E030120-01; 1:4,000; EarthOx Life Sciences, Millbrae, CA, USA) at room temperature for 30 min. Detection of protein bands was performed using the enhanced chemiluminescence for western blotting kit (Beyotime Institute of Biotechnology) according to the manufacturer's protocol. GAPDH or Lamin A was used as an internal control. Relative protein expression was determined by densitometry using Image J2x analysis software (National Institutes of Health, Bethesda, MD, USA).

Statistical analysis. All experiments were repeated three times. Data are presented as the mean ± standard error of the mean. Statistical analysis was performed with SPSS version 17.0 software (SPSS, Inc., Chicago, IL, USA). Differences between groups were initially evaluated using one-way analysis of variance, and multiple comparison analysis was further performed in the case that differences were statistically significant using Fisher's least significant difference test. P<0.05 was considered to indicate a statistically significant difference.

Results

GAS5 expression is induced by PA treatment in H9c2 myocardial cells. Oil Red O staining illustrated that lipids were accumulated in H9c2 cells following treatment with 400 μM PA (Fig. 1A), and the results of CCK-8 assay demonstrated that cell viability was markedly decreased by PA treatment (Fig. 1B), which suggested that PA induced lipotoxic injury in cardiomyocytes. In addition, the pro-inflammatory cytokine TNF-α and IL-1β mRNA and protein levels were significantly increased by PA treatment in H9c2 cells, as compared with the control group (Fig. 1C and D). This further suggests that PA exposure caused inflammation. Furthermore, the results of RT-qPCR revealed
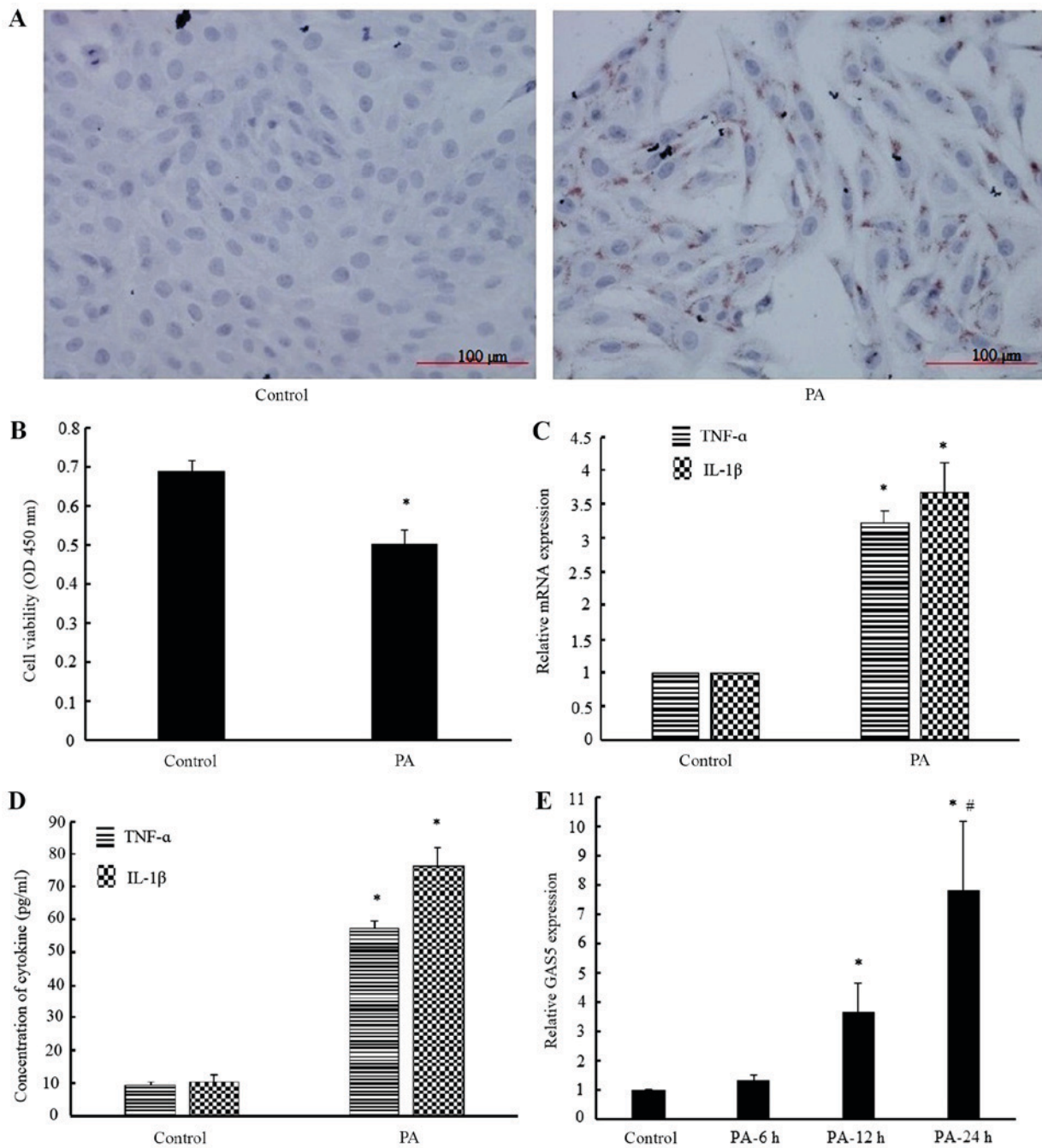
Figure 1. Expression of GAS5 in H9c2 cardiomyocytes treated with 400 μM PA for 24 h. (A) Cells were stained with Oil Red O solution and images were captured at x400 magnification. (B) Cell viability was determined by Cell Counting Kit-8 assay. (C) mRNA expression levels of TNF-α and IL-1β were detected by RT-qPCR. (D) Concentrations of TNF-α and IL-1β in culture medium were detected by enzyme-linked immunosorbent assay. (E) GAS5 expression in H9c2 cells was detected by RT-qPCR following treatment with 400 μM PA for 6, 12 or 24 h. Data are presented as the mean ± standard error from three independent experiments. *$P<0.05$ vs. control group; #$P<0.05$ vs. PA-12 h group. GAS5, growth arrest-specific transcript 5; PA, palmitic acid; TNF-α, tumor necrosis factor α; IL-1β, interleukin-1β; RT-qPCR, reverse transcription-quantitative polymerase chain reaction; OD, optical density.

that the expression of GAS5 in H9c2 cells was significantly increased by 3.65- and 7.82-fold following treatment with 400 μM PA for 12 and 24 h, respectively (Fig. 1E). Therefore, these results demonstrated that GAS5 expression was induced by PA treatment in H9c2 myocardial cells.

Knockdown of GAS5 expression alleviates PA-induced myocardial injury. The expression of GAS5 in H9c2 cells was reduced by nearly 70% following transfection with GAS5-specific siRNA (Fig. 2A), suggesting that GAS5

siRNA effectively inhibited the endogenous expression of GAS5 in cardiomyocytes. It was further observed that the cell viability was markedly increased (Fig. 2B) and the activity of LDH was significantly decreased by the downregulation of GAS5 in PA-treated cells (Fig. 2C). Taken together, these results demonstrated that the knockdown of GAS5 expression alleviated PA-induced myocardial injury.

Knockdown of GAS5 expression inhibits PA-induced inflammation. To evaluate whether GAS5 regulated PA-induced
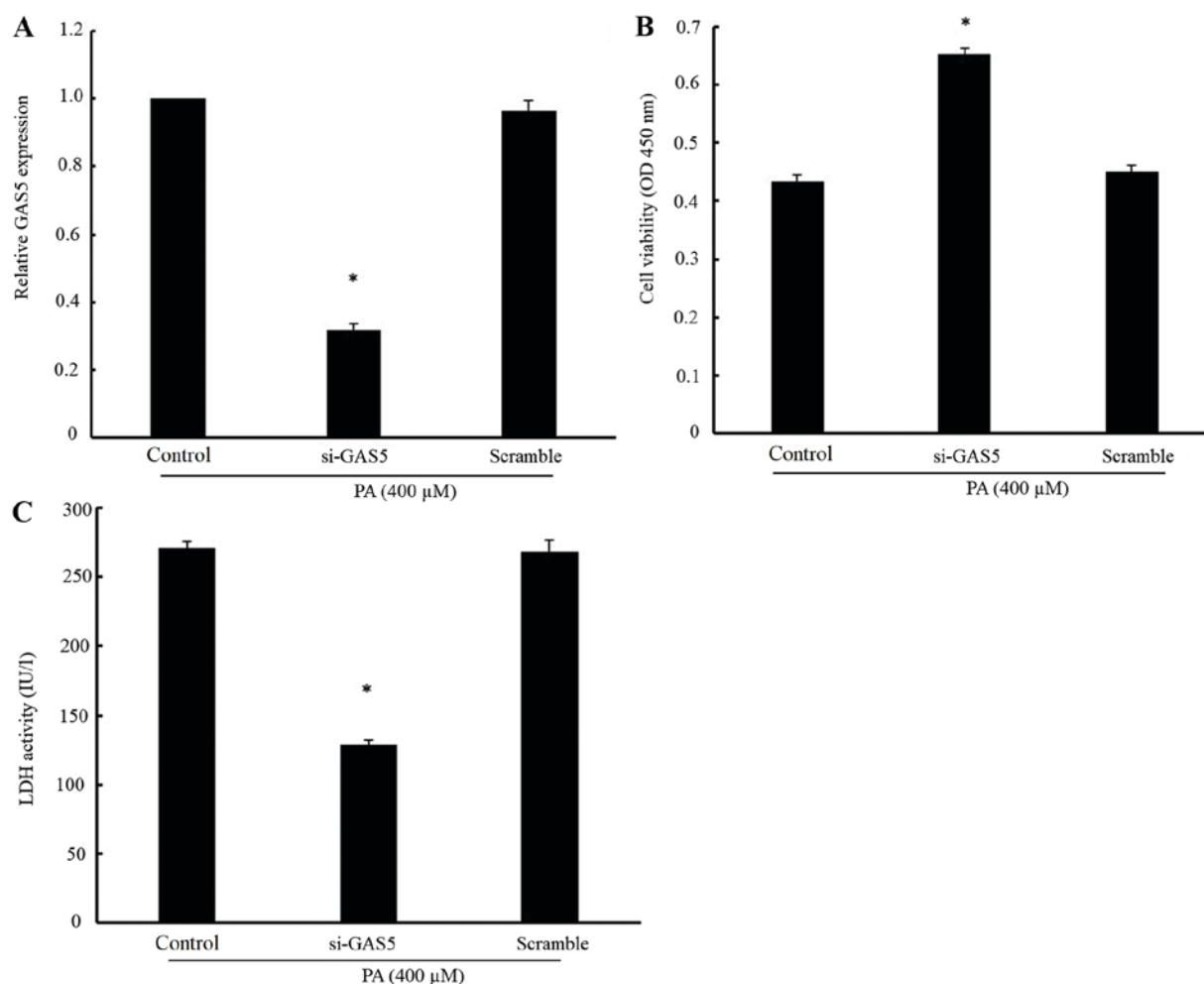
Figure 2. Effect of GAS5 expression knockdown on PA-induced myocardial injury. si-GAS5 and negative control (scramble) were transfected into H9c2 cells for 24 h, and cells were then treated with 400 μM PA for 24 h. Cells just treated with transfection reagents were used as a control. (A) GAS5 expression in H9c2 cells was detected by reverse transcription-quantitative polymerase chain reaction. (B) Cell viability was determined by Cell Counting Kit-8 assay. (C) LDH activity in the culture medium was detected by spectrophotometry. Data are presented as the mean ± standard error from three independent experiments. *P<0.05 vs. control group. GAS5, growth arrest-specific transcript 5; PA, palmitic acid; si-GAS5, GAS5-specific small interfering RNA; OD, optical density; LDH, lactate dehydrogenase.

inflammation, the present study detected the mRNA expression and concentration levels of the pro-inflammatory cytokines TNF-α and IL-1β. The results demonstrated that the mRNA expression levels of TNF-α and IL-1β in PA-treated H9c2 cells were notably reduced by the downregulation of GAS5 as compared with the non-transfected PA-treated group (Fig. 3A and B). In addition, the concentrations of TNF-α and IL-1β in PA-treated H9c2 cells were significantly decreased by the downregulation of GAS5 (Fig. 3C and D). Taken together, these results demonstrated that the downregulation of GAS5 inhibits PA-induced inflammation.

Interaction between GAS5 and miR-26a. Bioinformatics analysis (starBase v2.0; http://starbase.sysu.edu.cn/index. php) revealed that the GAS5 transcript sequence contained a miR-26a binding region (Fig. 4A). Subsequently, the results of the luciferase activity assay demonstrated that luciferase activity in the pmirGLO-GAS5 group was reduced by 61% in the group transfected with miR-26a mimics compared with mimics NC (Fig. 4B). In the pmirGLO-GAS5-mut group, miR-26a mimics did not have a significant inhibitory effect

on luciferase activity when compared with the mimics NC (Fig. 4B). These results demonstrated that GAS5 specifically binds with miR-26a.

Furthermore, the knockdown of GAS5 was demonstrated to markedly upregulate miR-26a expression, while treatment with miR-26a inhibitor significantly increased GAS5 expression (Fig. 4C and D). Therefore, these results further demonstrated that a reciprocal negative regulation exists between miR-26a and GAS5.

Knockdown of GAS5 expression inhibits HMGB1/NF-κB signaling mediated by miR-26a. As HMGB1 is a known target of miR-26a (24), the present study investigated whether GAS5, acting as a ceRNA, regulated the expression of HMGB1, and examined whether the regulation of GAS5 on the expression of HMGB1 was mediated by miR-26a. The results demonstrated that the mRNA and protein expression levels of HMGB1 were repressed by transfection with the GAS5-specific siRNA alone in PA-treated cells. However, co-transfection with the GAS5-specific siRNA and miR-26a inhibitor prevented the inhibition of the mRNA and protein expression levels
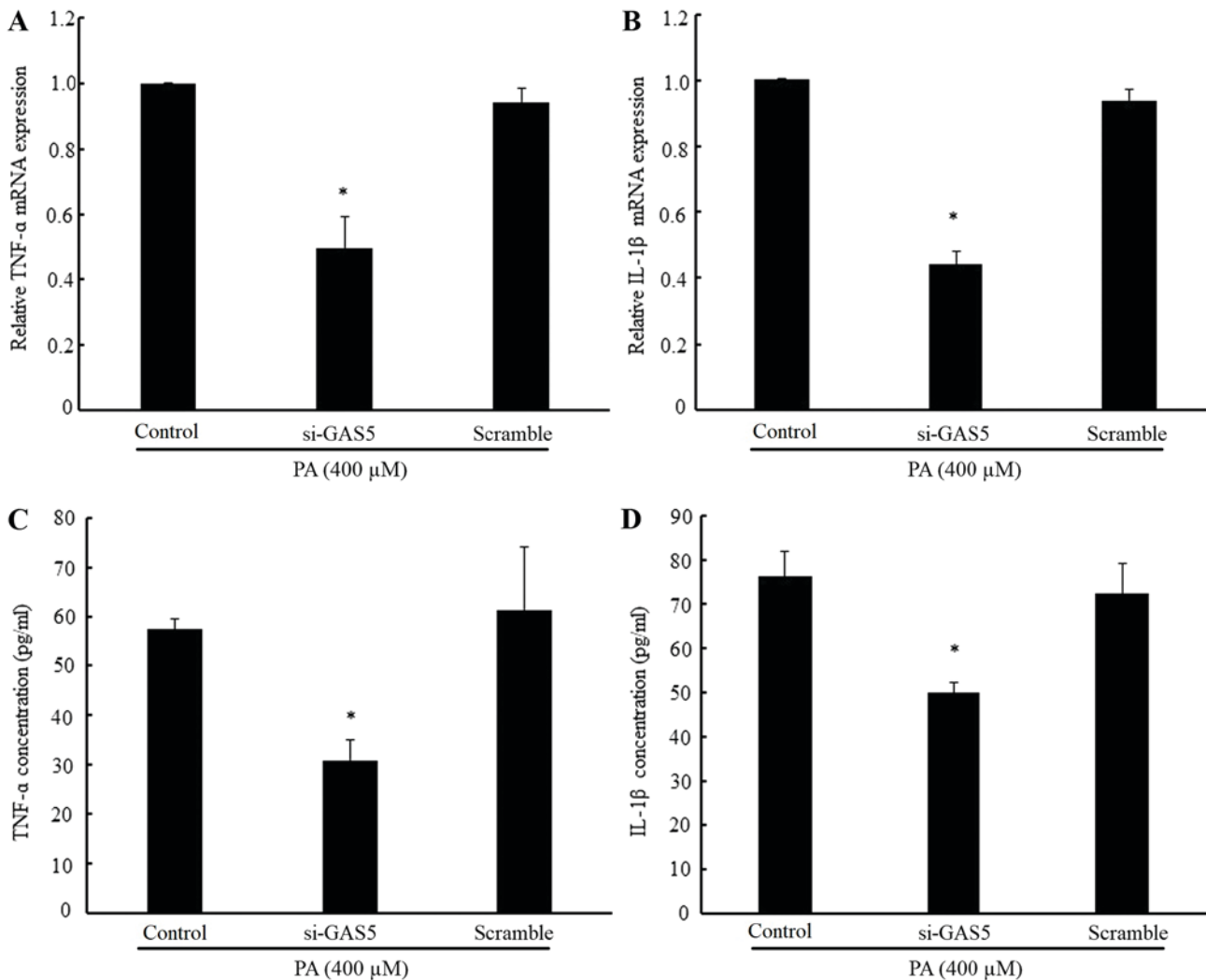
Figure 3. Effect of GAS5 downregulation on PA-induced inflammation. si-GAS5 and negative control (scramble) were transfected into H9c2 cells for 24 h, and cells were then treated with 400 μM PA for 24 h. Cells just treated with transfection reagents were used as a control. (A) TNF-α and (B) IL-1β mRNA expression levels were detected by reverse transcription-quantitative polymerase chain reaction. (C) TNF-α and (D) IL-1β concentrations in the culture medium were detected by enzyme-linked immunosorbent assay. Data are presented as the mean ± standard error from three independent experiments. *P<0.05 vs. control group. GAS5, growth arrest-specific transcript 5; PA, palmitic acid; si-GAS5, GAS5-specific small interfering RNA; TNFα, tumor necrosis factor α; Il-1β, interleukin-1β.

of HMGB1 (Fig. 5A and B). Similarly, transfection with the GAS5-specific siRNA alone decreased the protein expression of NF-κB in the nucleus, increased the cytoplasmic protein expression of NF-κB and inhibited the activity of NF-κB in cardiomyocytes. However, these effects of GAS5 knockdown on NF-κB were abolished by co-transfection with the miR-26a inhibitor (Fig. 5C and D). Taken together, these results demonstrated that the knockdown of GAS5 expression inhibited the HMGB1/NF-κB signaling pathway, and this effect was mediated by miR-26a.

Discussion

In the present study, the expression and role of GAS5 on PA-induced myocardial injury were examined. Previous studies have revealed that lncRNAs serve a regulatory role in cell and tissue damage induced by PA irritation (21,22,25,26). It has also been demonstrated that lncRNA hypoxia-inducible factor 1α-antisense RNA 1 (HIF1A-AS1) expression

is upregulated in vascular smooth muscle cells and human vascular endothelial cells exposed to PA, and that downregulation of HIF1A-AS1 expression reduced PA-induced apoptosis in these cells (25,26). However, the regulatory role of lncRNAs in PA-induced myocardial injury remains unknown. To the best of our knowledge, the present study is the first to report the role of lncRNAs in PA-induced myocardial injury.

GAS5 is typically induced under conditions of cellular stress, such as ischemia (17) and serum starvation (27). PA is an inducer of cellular oxidative stress and endoplasmic reticulum stress (22). As hypothesized, when rat myocardial H9c2 cells were exposed to PA, the expression levels of GAS5 were increased in the present study. Furthermore, it was demonstrated that the downregulation of GAS5 alleviated the extent of PA-induced myocardial injury. Taken together, the results of the present study suggest that GAS5 may be a novel putative therapeutic target for PA-induced myocardial injury.
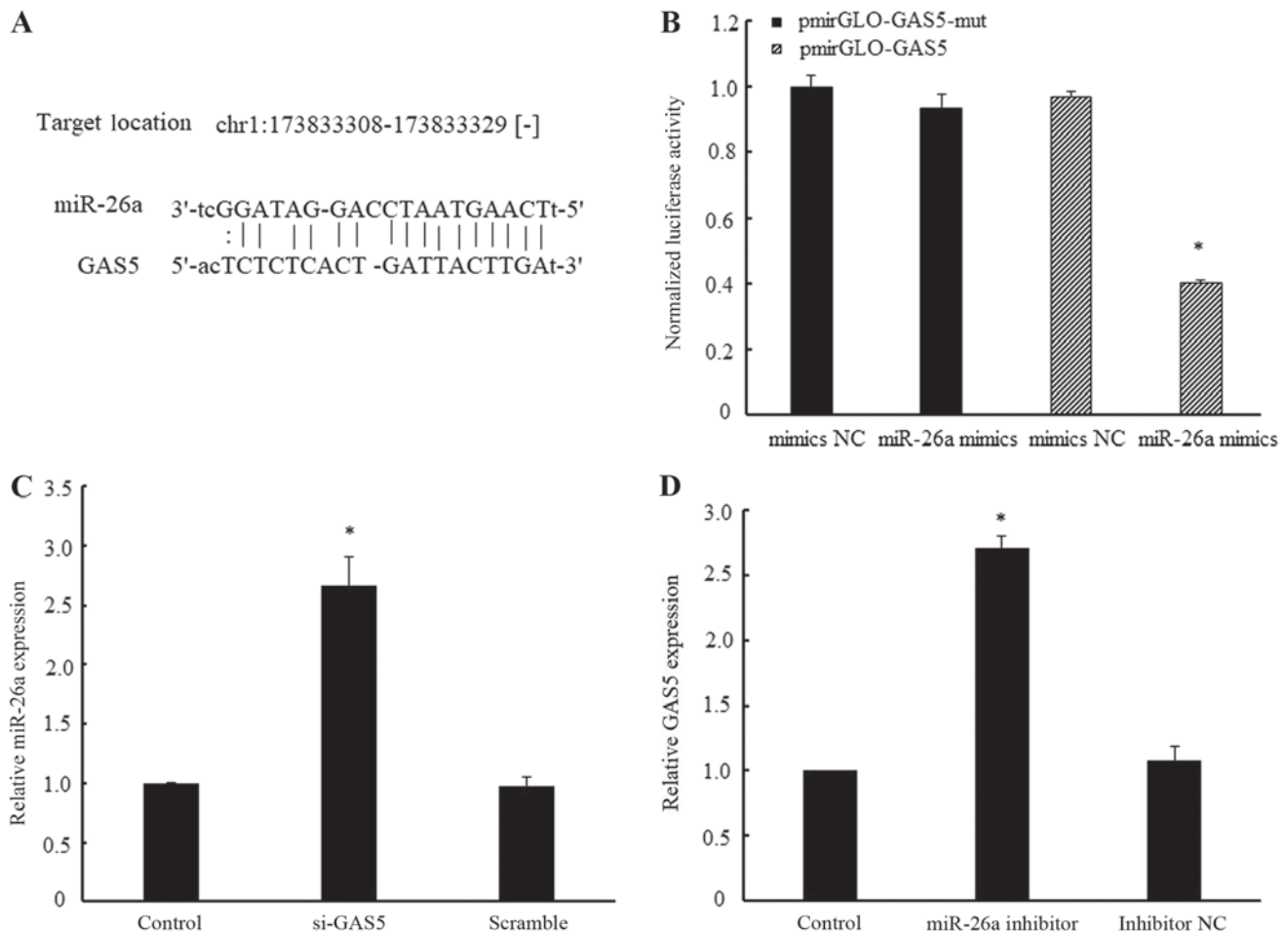
Figure 4. Interaction between GAS5 and miR-26a. (A) miRNA binding sites in the GAS5 sequence. (B) Luciferase reporter gene assay validated the interaction between GAS5 and miR-26a in H9c2 cells. pmirGLO-GAS5 served as the luciferase vector of GAS5, while pmirGLO-GAS5-mut was the GAS5 mutant vector. (C) Effect of GAS5 knockdown on the level of miR-26a. (D) Effect of miR-26a inhibition on the level of GAS5. Data are presented as the mean ± standard error from three independent experiments. *P<0.05 vs. mimics NC or control group. GAS5, growth arrest-specific transcript 5; NC, negative control; miR, microRNA.

Recent studies have provided growing evidence that PA-induced myocardial injury is associated with the activation of inflammatory and innate immune responses (5,6). PA may promote the development of myocardial injury through a mechanism of direct interactions with myeloid differentiation protein 2 and a Toll-like receptor 4 (TLR4) accessory protein, resulting in the activation of the TLR4/NF-κB signaling pathway for the regulation of pro-inflammatory molecules (5). GAS5 is a repressor of the glucocorticoid receptor (GR) through binding to its DNA-binding domain by acting as a molecular decoy (27). Furthermore, decreasing GAS5 levels can enhance the suppressive effect of glucocorticoid on inflammatory responses (28). As hypothesized, the current study revealed that the downregulation of GAS5 decreased the mRNA expression levels and activities of TNF-α and IL-1β in PA-treated myocardial cells. Thus, these results strengthen the evidence that GAS5 is a modulator of inflammatory response.

The regulatory type of lncRNA for gene function typically depends on its cellular location. The majority of lncRNAs in the cytoplasm regulate gene expression by sponging with miRNAs, functioning as ceRNAs (29). Several studies have demonstrated that GAS5 is abundantly expressed in the cytoplasm and regulates gene expression in a ceRNA regulatory mechanism (15,18). For instance, GAS5 has been reported to increase p27 expression as a ceRNA for miR-222, thereby inhibiting liver fibrosis progression (18). Thus, it is hypothesized that GAS5 may form a regulatory network of ceRNAs to regulate PA-induced myocardial injury. The present study demonstrated that GAS5 binds to miR-26a, and that a reciprocal negative regulation exists between miR-26a and GAS5. These results provide novel evidence for the interaction between miR-26a and GAS5.

HMGB1, a well-established miR-26a target gene, can activate NF-κB and increase the expression of pro-inflammatory cytokines (24). Therefore, in the present study, it was speculated that GAS5 functions as a ceRNA to regulate HMGB1 expression by binding with miR-26a. The results demonstrated that the downregulation of GAS5 inhibited the activation of the HMGB1/NF-κB signaling pathway, and this repressive effect was mediated by miR-26a. Taken together, the results of the present study demonstrated that GAS5 regulates HMGB1 expression through miR-26a binding, thereby inhibiting the activation of NF-κB.

However, there are limitations to the present research. The expression and role of GAS5 on PA-induced myocardial injury
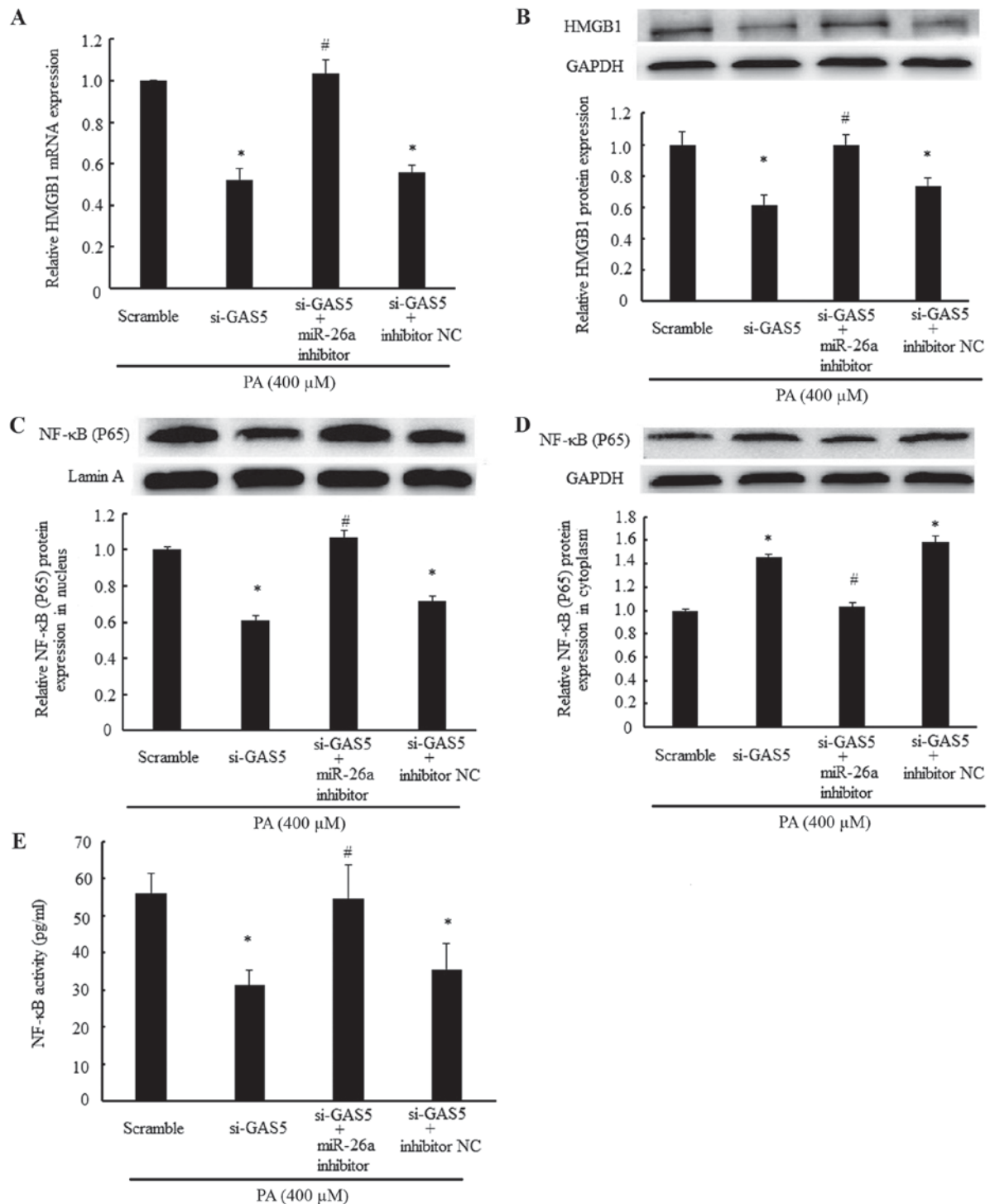
Figure 5. GAS5 regulates HMGB1 expression, and its effect is mediated by miR-26a. Scramble) and si-GAS5 transfection alone or together with miR-26a inhibitor or inhibitor NC was conducted in H9c2 cells for 24 h, and then cells were treated with 400 μM PA for 24 h. (A) mRNA and (B) protein expression levels of HMGB1 were detected by reverse transcription-quantitative polymerase chain reaction and western blotting, respectively. The protein expression of NF-κB (P65) in the (C) nucleus and (D) cytoplasm was detected by western blotting. (E) NF-κB activity was detected by ELISA. Data are presented as the mean ± standard error from three independent experiments. *P<0.05 vs. scramble group; #P<0.05 vs. si-GAS5 group. GAS5, growth arrest-specific transcript 5; HMGB1, high mobility group box 1; si-GAS5, GAS5-specific small interfering RNA; PA, palmitic acid.

was only confirmed *in vitro*. Therefore a myocardial lipotoxic injury *in vivo* model induced by PA or a high-fat diet should be used to further confirm the role of GAS5 in myocardial lipotoxic injury.

In conclusion, the present study demonstrated that GAS5 is upregulated in cardiomyocytes exposed to PA, while knockdown of GAS5 expression alleviates PA-induced myocardial inflammatory injury through the miR-26a/HMGB1/NF-κB axis. These findings provide a novel insight into the underlying mechanism of myocardial lipotoxic injury.

Acknowledgements

Availability of data and materials

All data generated or analyzed during this study are included in this published article.

Authors' contributions

QY, DJ and CM conceived and designed the experiments. QY and CZ conducted the experiments. YW, LZ, QZ and GL participated in the completion of the experiments. QY, LZ, QZ and GL analyzed the data. QY and NW wrote the paper. NW acquired and interpreted the data, and drafted and revised the manuscript. All the authors read and approved the final manuscript.

Ethics approval and consent to participate

Not applicable.

Patient consent for publication

Not applicable.

Competing interests

The authors declare that they have no competing interests.

References

1. NCD Risk Factor Collaboration (NCD-RisC): Worldwide trends in body-mass index, underweight, overweight, and obesity from 1975 to 2016: A pooled analysis of 2416 population-based measurement studies in 128·9 million children, adolescents, and adults. Lancet 390: 2627-2642, 2017.
2. Boden G: Obesity and free fatty acids. Endocrinol Metab Clin North Am 37: 635-646, viii-ix, 2008.
3. Djoussé L, Benkeser D, Arnold A, Kizer JR, Zieman SJ, Lemaitre RN, Tracy RP, Gottdiener JS, Mozaffarian D, Siscovick DS, et al: Plasma free fatty acids and risk of heart failure: The Cardiovascular Health Study. Circ Heart Fail 6: 964-969, 2013.
4. Zou L, Li X, Wu N, Jia P, Liu C and Jia D: Palmitate induces myocardial lipotoxic injury via the endoplasmic reticulum stress-mediated apoptosis pathway. Mol Med Rep 16: 6934-6939, 2017.
5. Wang Y, Qian Y, Fang Q, Zhong P, Li W, Wang L, Fu W, Zhang Y, Xu Z, Li X and Liang G: Saturated palmitic acid induces myocardial inflammatory injuries through direct binding to TLR4 accessory protein MD2. Nat Commun 8: 13997, 2017.
6. Zeng C, Zhong P, Zhao Y, Kanchana K, Zhang Y, Khan ZA, Chakrabarti S, Wu L, Wang J and Liang G: Curcumin protects hearts from FFA-induced injury by activating Nrf2 and inactivating NF-κB both in vitro and in vivo. J Mol Cell Cardiol 79: 1-12, 2015.
7. Sun W, Yang Y, Xu C and Guo J: Regulatory mechanisms of long noncoding RNAs on gene expression in cancers. Cancer Genet 216-217: 105-110, 2017.
8. Ratajczak MZ, Shin DM, Schneider G, Ratajczak J and Kucia M: Parental imprinting regulates insulin-like growth factor signaling: A Rosetta Stone for understanding the biology of pluripotent stem cells, aging and cancerogenesis. Leukemia 27: 773-779, 2013.
9. Lee JT: The X as model for RNA's niche in epigenomic regulation. Cold Spring Harb Perspect Biol 2: a003749, 2010.
10. Hung T, Wang Y, Lin MF, Koegel AK, Kotake Y, Grant GD, Horlings HM, Shah N, Umbricht C, Wang P, et al: Extensive and coordinated transcription of noncoding RNAs within cell-cycle promoters. Nat Genet 43: 621-629, 2011.
11. Sen R, Ghosal S, Das S, Balti S and Chakrabarti J: Competing endogenous RNA: The key to posttranscriptional regulation. ScientificWorldJournal 2014: 896206, 2014.
12. Ji P, Diederichs S, Wang W, Böing S, Metzger R, Schneider PM, Tidow N, Brandt B, Buerger H, Bulk E, et al: MALAT-1, a novel noncoding RNA, and thymosin beta4 predict metastasis and survival in early-stage non-small cell lung cancer. Oncogene 22: 8031-8041, 2003.
13. Wang Y, Zhang Y, Yang T, Zhao W, Wang N, Li P, Zeng X and Zhang W: Long non-coding RNA MALAT1 for promoting metastasis and proliferation by acting as a ceRNA of miR-144-3p in osteosarcoma cells. Oncotarget 8: 59417-59434, 2017.
14. Coccia EM, Cicala C, Charlesworth A, Ciccarelli C, Rossi GB, Philipson L and Sorrentino V: Regulation and expression of a growth arrest-specific gene (gas5) during growth, differentiation, and development. Mol Cell Biol 12: 3514-3521, 1992.
15. Zhang Z, Zhu Z, Watabe K, Zhang X, Bai C, Xu M, Wu F and Mo YY: Negative regulation of lncRNA GAS5 by miR-21. Cell Death Differ 20: 1558-1568, 2013.
16. Ma C, Shi X, Zhu Q, Li Q, Liu Y, Yao Y and Song Y: The growth arrest-specific transcript 5 (GAS5): A pivotal tumor suppressor long noncoding RNA in human cancers. Tumour Biol 37: 1437-1444, 2016.
17. Chen F, Zhang L, Wang E, Zhang C and Li X: LncRNA GAS5 regulates ischemic stroke as a competing endogenous RNA for miR-137 to regulate the Notch1 signaling pathway. Biochem Biophys Res Commun 496: 184-190, 2018.
18. Yu F, Zheng J, Mao Y, Dong P, Lu Z, Li G, Guo C, Liu Z and Fan X: Long Non-coding RNA growth arrest-specific transcript 5 (GAS5) inhibits liver fibrogenesis through a mechanism of competing endogenous RNA. J Biol Chem 290: 28286-28298, 2015.
19. Tao H, Zhang JG, Qin RH, Dai C, Shi P, Yang JJ, Deng ZY and Shi KH: LncRNA GAS5 controls cardiac fibroblast activation and fibrosis by targeting miR-21 via PTEN/MMP-2 signaling pathway. Toxicology 386: 11-18, 2017.
20. Song J, Ahn C, Chun CH and Jin EJ: A long non-coding RNA, GAS5, plays a critical role in the regulation of miR-21 during osteoarthritis. J Orthop Res 32: 1628-1635, 2014.
21. Yan C, Chen J and Chen N: Long noncoding RNA MALAT1 promotes hepatic steatosis and insulin resistance by increasing nuclear SREBP-1c protein stability. Sci Rep 6: 22640, 2016.
22. Brookheart RT, Michel CI, Listenberger LL, Ory DS and Schaffer JE: The non-coding RNA gadd7 is a regulator of lipid-induced oxidative and endoplasmic reticulum stress. J Biol Chem 284: 7446-7454, 2009.
23. Livak KJ and Schmittgen TD: Analysis of relative gene expression data using real-time quantitative PCR and the 2(-Delta Delta C(T)) method. Methods 25: 402-408, 2001.
24. Yao L, Lv X and Wang X: MicroRNA 26a inhibits HMGB1 expression and attenuates cardiac ischemia-reperfusion injury. J Pharmacol Sci 131: 6-12, 2016.
25. He Q, Tan J, Yu B, Shi W and Liang K: Long noncoding RNA HIF1A-AS1A reduces apoptosis of vascular smooth muscle cells: Implications for the pathogenesis of thoracoabdominal aorta aneurysm. Pharmazie 70: 310-315, 2015.
26. Wang J, Chen L, Li H, Yang J, Gong Z, Wang B and Zhao X: Clopidogrel reduces apoptosis and promotes proliferation of human vascular endothelial cells induced by palmitic acid via suppression of the long non-coding RNA HIF1A-AS1 in vitro. Mol Cell Biochem 404: 203-210, 2015.
27. Kino T, Hurt DE, Ichijo T, Nader N and Chrousos GP: Noncoding RNA gas5 is a growth arrest- and starvation-associated repressor of the glucocorticoid receptor. Sci Signal 3: ra8, 2010.
28. Keenan CR, Schuliga MJ and Stewart AG: Pro-inflammatory mediators increase levels of the noncoding RNA GAS5 in airway smooth muscle and epithelial cells. Can J Physiol Pharmacol 93: 203-206, 2015.
29. Rashid F, Shah A and Shan G: Long non-coding RNAs in the cytoplasm. Genomics Proteomics Bioinformatics 14: 73-80, 2016.